Eur. Phys. J. B **31**, 195–202 (2003)
DOI: 10.1140/epjb/e2003-00023-9

THE EUROPEAN PHYSICAL JOURNAL B

Transverse magnetic susceptibility of thin films and multilayers exhibiting perpendicular anisotropy

M. Labrune[1,a] and H. Niedoba[2]

[1] Laboratoire PMTM-CNRS, Université Paris 13, 93430 Villetaneuse, France
[2] Laboratoire de Magnétisme et d'Optique de Versailles[b] , UVSQ 78035 Versailles, France

Received 10 October 2002
Published online 4 February 2003 –

Abstract. A full analysis of domain structure using a micromagnetic model is developed in order to get a clear insight into the behaviour of transverse initial susceptibility as a function of dc applied field for thin films and bilayers exhibiting both in-plane and perpendicular anisotropy. The numerical simulations are in good agreement with available experimental results in case of single layers with the so-called stripe domain pattern while some predictions are done for bilayers. As the main result, it is shown that in low field, the transverse initial susceptible cannot be interpreted without the knowledge of the static domain pattern while, above saturation, it is only affected by the in-plane anisotropy.

PACS. 75.40.Cx Static properties (order parameter, static susceptibility, heat capacities, critical exponents, etc.) – 75.60.Ch Domain walls and domain structure – 75.70.Cn Interfacial magnetic properties (multilayers, superlattices) – 75.50.Ss Magnetic recording materials

1 Introduction

The technique of transverse biased initial susceptibility (TBIS) measurement [1] using magneto-optical effects (Kerr effect, [2]) has proved to be a very sensitive tool to characterize magnetic properties especially to determine macroscopic and local anisotropy fields. From the experimental point of view, a small alternating (low frequency $f \approx 50$ Hz) field $\mathbf{h}$ and an orthogonal steady field $\mathbf{H}$, both in the sample plane are applied. The transverse susceptibility χ_t, measured along the ac field direction as a function of H, is defined as:

$$\chi_t = \lim_{\delta h \to 0} \frac{\delta M_t}{\delta h}$$

where δM_t is the elementary variation of the magnetization component induced along the small ac field caused by δh.

A lot of experimental work has been done so far on single films [2,3] or ultra-thin films [4], multilayers [5] as well as nanostructures [6] for both in-plane and perpendicular anisotropy.

In case of an uniaxial in-plane anisotropy, and as far as a single magnetic layer is considered, the basic results may be easily established in the framework of the coherent rotation model of Stoner and Wohlfarth in which only a single domain state is considered. Starting from the saturated state and under a decreasing field H applied at an angle β, the equilibrium magnetization orientation referenced by θ_0 ($\theta_0 \leq \beta \leq \frac{\pi}{2}$, both angles are measured with respect to the easy axis) is given by:

$$K_{\text{plan}} \sin(2\theta_0) + HM \sin(\theta_0 - \beta) = 0 \qquad (1)$$

corresponding to the nullity of the first derivative of the free energy with respect to θ.

Therefore, the transverse susceptibility is equal to:

$$\chi_t = \frac{M^2 \cos^2(\theta_0 - \beta)}{2K_{\text{plan}} \cos(2\theta_0) + HM \cos(\theta_0 - \beta)} \qquad (2)$$

where K_{plan} and M are the in-plane anisotropy constant and the saturation magnetization respectively. In fact, only two geometries are experimentally used. The first one corresponds to the d.c. field $\mathbf{H}$ applied along the easy direction ($\beta = 0$) where equation (2) reduces to $1/\chi_t = (H + H_{Kp})/M$, with $H_{Kp} = 2K_{\text{plan}}/M$. In the second situation, where $\mathbf{H}$ is along the hard axis ($\beta = \pi/2$) the inverse susceptibility reads either $1/\chi_t = (H - H_{Kp})/M$ for $H > H_{Kp}$ or $1/\chi_t = \frac{H_{Kp}}{M}(1-\alpha^2)/\alpha^2$, with $\alpha = H/H_{Kp}$ for $H < H_K$. These two situations are shown in Figure 1 and are effectively observed in thin amorphous films with in-plane anisotropy (*e.g.* CoZrTb film in Ref. [7]). But such a theoretical behaviour leading to a linear variation of $1/\chi_t$ with $\mathbf{H}$ is not exactly followed in polycrystalline soft magnetic films where the magnetization is no longer uniform in direction due to ripple structure. Hoffmann [8,9] developed a theory of transverse bias initial susceptibility in order to explain such deviation which

[a] e-mail: ml@lpmtm.univ-paris13.fr
[b] UMR CNRS 8634

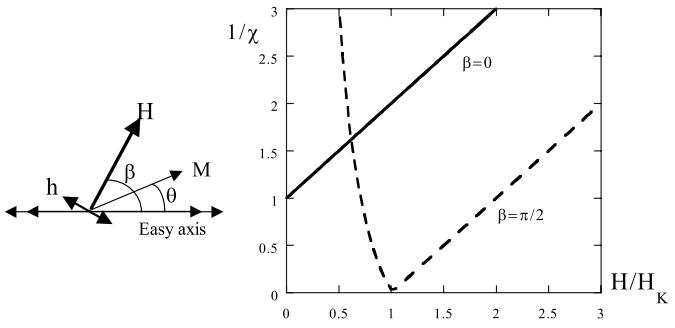

Fig. 1. Variation of χ_t^{-1} (in unit of H_K/M) *versus* the applied dc field **H** when this field along the easy axis $\beta = 0$ or along the hard axis $\beta = \pi/2$. Case of a thin film with uniaxial in-plane anisotropy (Stoner-Wohlfarth model).

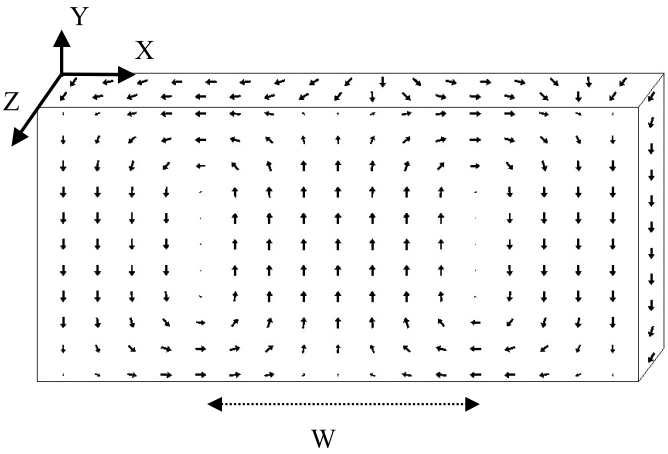

Fig. 2. Geometry and 3D magnetization profiles over one period $2W$ of a single film.

includes two supplementary contributions: one from short-range fluctuation and a second one: the so-called "skew" term caused by long-range fluctuations of induced magnetic anisotropy. It should be stressed that the Hoffmann's model is valid only for an applied field larger than the saturation field and only when M lies in the film plane. It can be mentioned here that the transverse susceptibility is also a powerful tool to analyse small perturbations from the predicted uniformly magnetized state due to the small size of samples such as nanomagnets and represents a good way to analyse the dependence of the energy on the magnetization direction [10].

More recently, experimental results of the behaviour of the transverse susceptibility for thin films [2,7,11,12] and multilayers [5] exhibiting perpendicular anisotropy ($K_{\rm per}$ will indicate the perpendicular anisotropy constant in what follows) have been published. However, for a dc field lower than the saturation field a stripe domain pattern occurs (see Fig. 2 for example). For such materials, the coherent rotation model of Stoner and Wohlfarth is, of course, no more sufficient and the spin dynamics of non-uniform magnetization distribution, which is a very attractive topic, should be taken into account. But the interpretation of these results is no longer straightforward. Therefore, some glorious mistakes (confusions) occurred in the literature so far. For example in reference [7] where the influence of the magnetic pattern is not taken into account, a quality factor $Q = K_{\rm per}/2\pi M_s^2$ in excess of 1 is needed to fit the experimental TBIS results for CoNbZr films. This obviously is not the case for samples used which, as we show in this paper, behave similar to amorphous CoFeZr thin films with stripe domains [13]. The first more satisfactory theoretical approach to explain TBIS behaviour including stripe domains is due to Alvarez-Prado *et al.* [5] in the case of a single film. They propose a quasistatic model with a sine-wave profile for M to explain the behaviour when stripes are present. Then, under the bias field action, two extreme cases are calculated: either all the moments are identically rotated toward the applied bias field or the magnetization rotation follows the condition div$\mathbf{M} = 0$.

The aim of this paper is to study theoretically the influence of a perpendicular anisotropy on the transverse susceptibility both in single films and in bilayer system taking into account a 3D magnetization distribution in stripe domains described earlier [14]. Predictive results are given for single films and bilayers, with the help of micromagnetic simulations, assuming a perpendicular anisotropy strong enough to support a weak stripe pattern even with no interlayer exchange coupling for bilayer systems.

2 Single layer exhibiting perpendicular anisotropy: CoNbZr

The first part of this study is devoted to a single film of CoNbZr 210 nm thick. The magnetization obtained by VSM measurements amounts to $4\pi M_S = 9000$ G. On the other hand, the in-plane VSM hysteresis loops are characteristic of a sample exhibiting both a weak perpendicular anisotropy and also some in-plane contribution. Along the in-plane easy direction, the saturation field $H_{\rm sat}$ and the remanent magnetization M_R amount to $H_{\rm sat} = 56$ Oe. and $M_R/M_S = 0.74$ respectively. These values are equal to $H_{\rm sat} = 60$ Oe. and $M_R/M_S = 0.71$ along the in-plane hard direction. The zero-field magnetic structure of the film has been investigated by Magnetic force microscopy (dimension 3100 apparatus). We used CoCr-coated Si cantilevers supplied by Digital, with the tips magnetized along their axis (perpendicular to the sample surface). The interlaced mode developed by Digital Instrument was used for the magnetic measurement. In this mode each line is scanned twice. The first scan records topographic information. For the second scan, on the same line, the cantilever is lifted (at the height of 50 nm in the present work) and the magnetic information is deduced from long range magnetic forces. These forces are measured using the phase detection system which measures the cantilever's phase oscillation relative to the piezo drive due to resonant frequency shifts. The signal is expected to be proportional to the second derivative *versus* Y (normal to the film plane) of the normal component of the stray field B_y at the tip position. Figure 3 shows one MFM image which reveals a well-defined stripe pattern of average period $2W = 400$ nm.

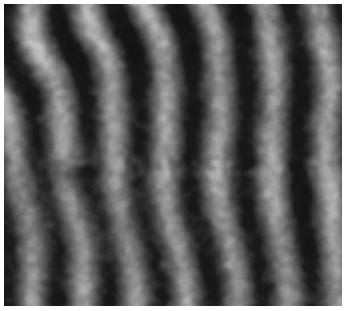

Fig. 3. MFM domain pattern for CoNbZr, image relative to (2.8×2.6 μm^2) sample area.

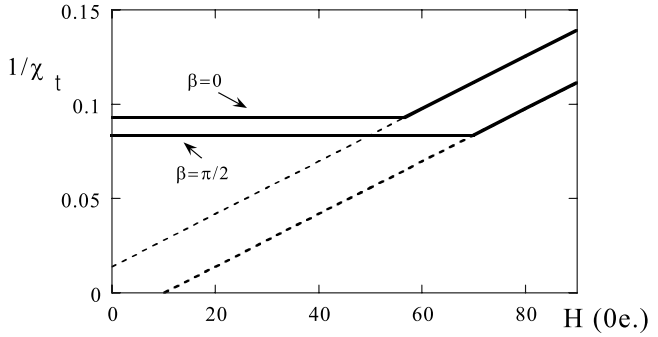

Fig. 4. Variation of the inverse susceptibility $1/\chi_t$ *versus* the dc in-plane field H applied either parallel ($\beta = 0$) or perpendicular ($\beta = \pi/2$) to the in-plane easy axis in the case of the CoNbZr film.

According to the lift scan height [15,16] the bright and dark areas can be regarded as corresponding to the position of the inner up and down domains.

Numerical calculations have been performed with $A = 10^{-6}$ erg/cm^3, thickness $t = 210$ nm and $M_S = 717$ emu/cm^3. The micromagnetic code used in the present calculations is described in references [14] and [16]. The anisotropy energy density $E_{\rm ani}$ used is:

$$E_{\rm ani} = K_{\rm per}(1 - m_y^2) + K_{\rm plan}(1 - m_Z^2) \qquad (3)$$

where $\mathbf{m} = \mathbf{M}/M_S$, $K_{\rm per}$ is the perpendicular to the film anisotropy constant and $K_{\rm plan}$ the in-plane anisotropy the OZ axis being both the easy in-plane direction and that of elongation of the stripe pattern (see geometry Fig. 2).

The best agreement with regard to the experimental results is obtained for $K_{\rm per} = 1.3 \times 10^5$ erg/cm^3 and $K_{\rm plan} = 3.5 \times 10^3$ erg/cm^3. The following numerical results were got: for stripes parallel to the in-plane easy axis $2W = 396$ nm, $H_{\rm sat} = 56.6$ Oe. and $M_R/M_S = 0.74$ while $2W = 406$ nm, $H_{\rm sat} = 70$ Oe. and $M_R/M_S = 0.70$ respectively when the stripes are elongated along the hard axis. It is to be noticed that the quality factor value, $Q = 0.04$, is effectively low, as it was guessed from the in-plane hysteresis curves shape. With the set of numerical data given above, micromagnetic calculations were performed in order to obtain the transverse bias susceptibility. First, for a given static field H applied along the stripe, the equilibrium structure is searched and the equilibrium width of the domains: $W(H)$ is got. The very low frequency of the ac transverse field ($f \approx 50$ Hz) is far from any resonance area so that damping effect overcome any dynamical or precession contribution. Therefore, the action of the ac field can be analysed as a sequence of quasi-static equilibrium situations. Consequently, assuming a constant transverse field h and neglecting the h induced change in the period [$2W(\mathbf{H}) = 2W(\mathbf{H}+\mathbf{h})$],a new equilibrium magnetic pattern is found from which the transverse magnetization component is extracted. Several calculations are then performed with decreasing value of the transverse field h. The limit of the ratio: variation of the transverse magnetization over the field value h gives finally the transverse susceptibility χ_t. The inverse transverse susceptibily variation in function of the static H field is plotted in Figure 4. As one can observe in this figure, the inverse susceptibility is constant until the saturation is reached. For higher static field, it varies linearly according to the previous law mentioned in Section 1:

$$1/\chi_t = [H \pm 2K_{\rm plan}/M]/M. \qquad (4)$$

Compared to the experimental results published so far [2,7] on the same CoNbZr film, the following remarks can be made: for a dc applied field higher than the saturation field, the agreement is very good between experimental results and the modelisation assuming a coherent rotation model. But for lower field values ($H < Hk$), this model cannot be used any more. It is necessary to include the details of stripe domain configuration as done in this paper to get an agreement with the experimental results. This approach deeply differs from the interpretation given in references [2] and [7] where a uniformly magnetized sample is considered also for $H < Hk$ leading to a prohibitive value for the perpendicular anisotropy ($Q > 1$), in total disagreement with hysteresis loops and MFM observations. In conclusion, the transverse bias initial susceptibility method only gives informations on the in-plane anisotropy constant and on the saturation field. Access to the perpendicular anisotropy constant needs other experiments and extra numerical calculations as proposed in this paper.

In the following, we shall discuss the micromagnetic origin of the transverse biased initial susceptibility behaviour. In the saturated range, the evolution of the susceptibility is quite obvious. The stronger the applied field **H** is, the weaker the susceptibility is. In other words a strong dc field hardens the magnetic structure as it is maintaining the magnetization along its direction. On the contrary, in the non-saturated state a stripe pattern appears and such structure is less flexible compared to a uniformly magnetized sample. Now, one must also take into account wall displacements. In order to analyse the physical origin of such behaviour, results of micromagnetic calculations showing a non uniform magnetization rotation towards the transverse field h are given in Figure 5. Figure 5a is a crude magnetic representation of one period of the equilibrium state already depicted in Figure 2 while Figure 5b shows the variation of the modulus of the component m_X under the action of the small transverse

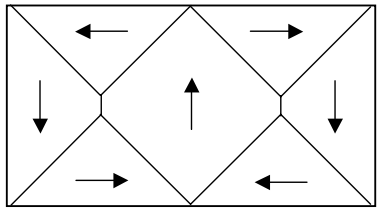

(a)

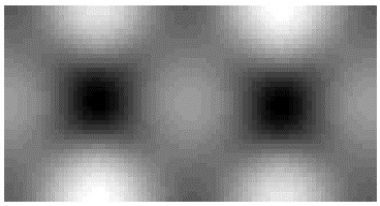

(b)

Fig. 5. a) Schematic magnetization distribution in cross section over one period of the equilibrium stripe pattern without any applied field and b) map of the modulus of the variation δm_X under the action of the small transverse ac field h also parallel to the X axis. (high levels in black and low levels in white).

ac field h (with respect to the zero field's one). Comparison between Figures 5a and b indicates that the maximum effect occurs in the inner part of the sample, especially in the middle of the 180° wall (its Bloch part, which can be assimilated to a vortex core; see Fig. 2). Otherwise, closure domains where M is along (or in the vicinity of) **h** expend while the others where M is opposite to h shrink according to Figure 6. This strain mode of vibration exists without any magnetostatic constrain. An order of magnitude of the transverse susceptibility (in absence of the dc field: $H = 0$) can be obtained within a very crude model in which the planar anisotropy, $K_{\rm plan}$, is neglected. Assuming in cross section a pure Landau structure (Fig. 5a) with inner 180° domains magnetized up and down along the perpendicular easy axis with closure domains at 90°, the equilibrium stripe width W is obtained by minimizing the total free energy including wall and anisotropy contributions. This calculation leads to the classical result for the domain width: $W = \sqrt{2\gamma_{180} t/K_{\rm per}}$, where γ_{180} is the 180° wall energy which can be estimated to be approximately equal to $4\sqrt{AK_{\rm per}}$. Under the action of a small transverse field h, the pattern is deformed according to Figure 6. Assuming the magnetic period constant: $2W = W_+ + W_-$, calculations, including this time the Zeeman term, lead to: $W_+ = W(1 + hM/K)$. The corresponding increase of magnetization δM, parallel to h over one magnetic period $2W$ is given by: $\delta M 2Wt = M(W_+^2 - W_-^2)/2$ what can be written as $\delta M = \frac{2M^2}{K_{\rm per}}(\frac{W}{t})h$ (with $H = 0$) and the inverse transverse susceptibility reads:

$$1/\chi_t = \frac{K_{\rm per}}{2M^2}\left(\frac{t}{W}\right). \qquad (6)$$

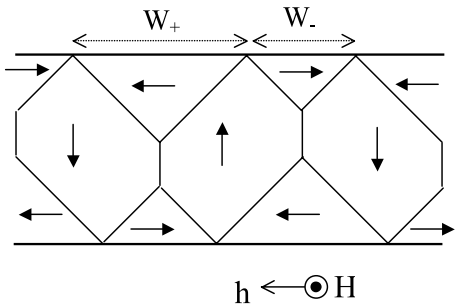

Fig. 6. Expected modification of the Landau pattern under the presence of a transverse field h.

Numerical calculation gives $1/\chi_t = 0.12$ in relatively good agreement with what is expected from numerical simulations and observed experimentally.

3 Single layers and bilayers with intermediate values of perpendicular anisotropy: general approach

Special attention is now paid to Co films and bilayers. A quality factor $Q = K_{\rm per}/2\pi M^2$ of the order of 0.4 is typical for thin epitaxial cobalt films [15] namely: magnetization $M = 1400$ emu/cc, perpendicular anisotropy $K_{\rm per} = 5 \times 10^6$ erg/cm^3, exchange constant $A = 1.8 \times 10^{-6}$ erg/cm. The possible occurrence of large perpendicular anisotropy makes Cobalt thin films and stacks attractive candidates for high data storage media [17]. In relation with this field of interest, this section is devoted first to the study of single films of Co.

3.1 Scale law

A large range of sample thickness t is used. In the simple case of a uniaxial perpendicular anisotropy, single magnetic films are fully characterized by three magnetic parameters: exchange A, anisotropy K and magnetization M plus one space parameter: the thickness of the sample t. Two characteristic lengths can be built: the Bloch length $\delta_K = 2\pi\sqrt{A/K}$ and the exchange one $\delta_{\rm ex} = 2\pi\sqrt{A/(2\pi M^2)}$. As the zero-field domain pattern is essentially controlled by two parameters: Q and one dimensionless ratio $R_H = t/\delta_K$ [18], the same magnetic behaviour should be expected for different samples assuming that these two parameters are kept constant, or equivalently if, from one sample to the other the two ratios t/δ_K and $t/\delta_{\rm ex}$, are preserved. Therefore if one dilates the thickness by a factor μ and the anisotropy by λ, the magnetization should in turn be increased by the factor $\sqrt{\lambda}$ while the exchange constant should be multiplied by $\lambda\mu^2$. Furthermore, two characteristic fields are used: the anisotropy field $H_K = 2K_{\rm per}/M$ and the dipolar field: $H_M = 4\pi M$ which both scale with $\sqrt{\lambda}$ and so does the applied field.

Table 1. Variation of the thickness over stripe-domain width: t/W, remanent magnetization in zero field and inverse transverse bias susceptibility either in zero dc applied field or near in-plane saturation. $K = 5 \times 10^6$ erg/cm^3, $A = 1.8 \times 10^{-6}$ erg/cm and $M_S = 1400$ emu/cc with $Q = 0.4$, $R_H = t/(2\pi\sqrt{A/K})$.

			$H = 0$		saturation	
R_H	t(nm)	t/W	M_z/M_s	$1/\chi_t$	H_{sat}/H_K	$1/\chi_t$
1.1	42	1	0.36	1.52	0.37	1.86
1.5	57	1.05	0.24	1.8	0.50	2.01
3	114	2.06	0.14	2.4	0.74	3.72
3.8	145	2.15	0.13	2.54	0.79	3.97

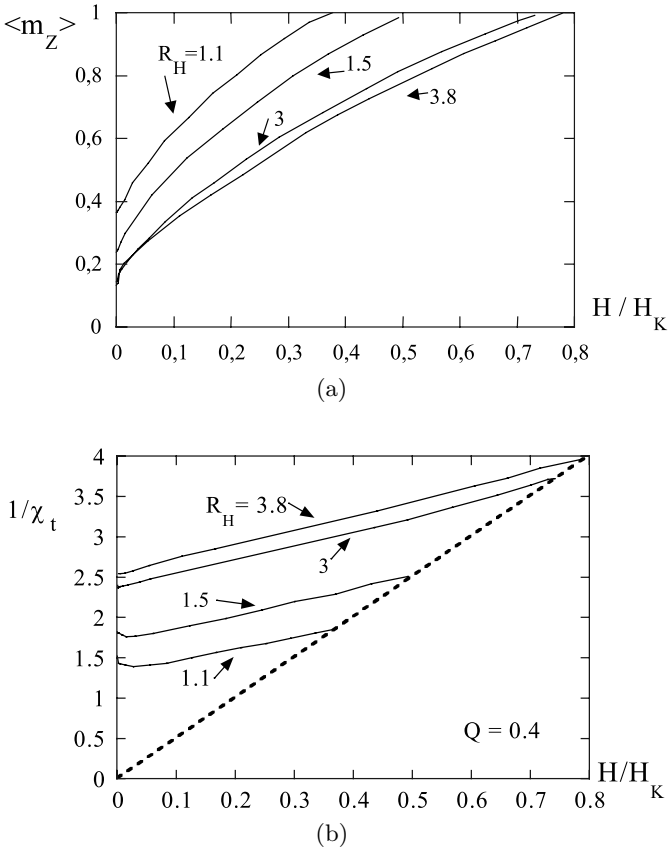

Fig. 7. (a) Variation of the longitudinal magnetization component and (b) of the inverse transverse bias susceptibility *versus* the dc applied field H, for different single films characterized by the same quality factor $Q = 0.4$ and various ratio factor R_H (see text). In Figure 7b, the dashed line corresponds to the expected behaviour for an applied field higher than the saturation field.

3.2 Numerical results for single films

Numerical results for four different thickness values are presented in Table 1. The variation of the longitudinal component $\langle m_Z \rangle$ as function of the in-plane dc field H is shown in Figure 7a while Figure 7b exhibits the corresponding variation of the inverse transverse susceptibility. Comparing $\langle m_Z \rangle$ and $1/\chi$, one can observed a relation between the inverse susceptibility and the mean magnetization: the smaller is $\langle m_Z \rangle$ for a given sample, the higher is its $1/\chi$ value. But for each sample, starting from zero field, $1/\chi$ increases regularly with $\langle m_Z \rangle$ until saturation is reached. Beyond this threshold field, $1/\chi$ varies linearly according to relation (4) which can be expressed as $1/\chi = H/M = 4\pi Q(H/H_K)$, (dashed line in Fig. 7). Furthermore, a small increase of $(\chi)^{-1}$ can be noticed near $H = 0$ for R_H values next to unity. For a vanishing applied field, $(\chi)^{-1}$ can be roughly estimated according to equation (6) which gives 1.25; 1.32; 2.58 and 2.7 for $R_H = 1.1$; 1.5; 3 and 3.8 respectively.

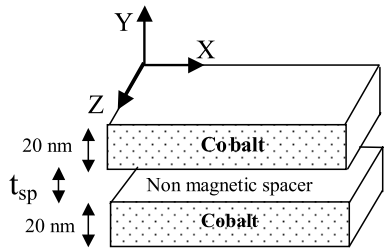

Fig. 8. Fig. 8: Bilayer geometry.

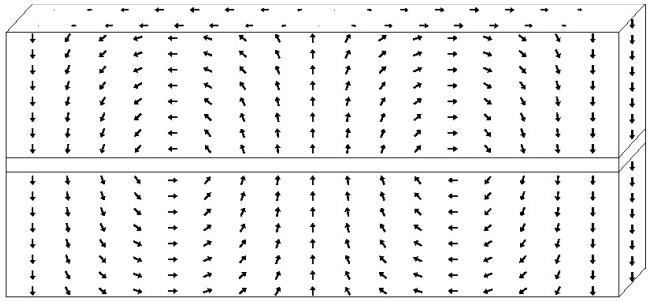

Fig. 9. 3d magnetization profiles over one period $2W$ of a bilayer (Co 20 nm/spacer 0.7 nm/Co 20 nm).

4 Bilayer system: [Co/spacer/Co]

4.1 Samples and geometry

This section is devoted to the study of the bilayer system composed of two cobalt layers 20 nm thick each separated by a non-magnetic spacer of varying thickness: t_{sp} ranging from 0.7 to 3.5 nm (Fig. 8). The magnetic parameters of cobalt sublayers are the same as those used previously in single films simulations based on [15] giving $Q = 0.4$. Therefore a stripe domain pattern is expected to occur. Such magnetic configuration is drawn in a particular case of $t_{sp} = 0.7$ nm in Figure 9 while a full and general description of stripe pattern occurring in bilayers can be obtained in reference [14].

4.2 Transverse susceptibility

The variation of the inverse transverse susceptibility versus the constant applied field H, parallel to the direction of

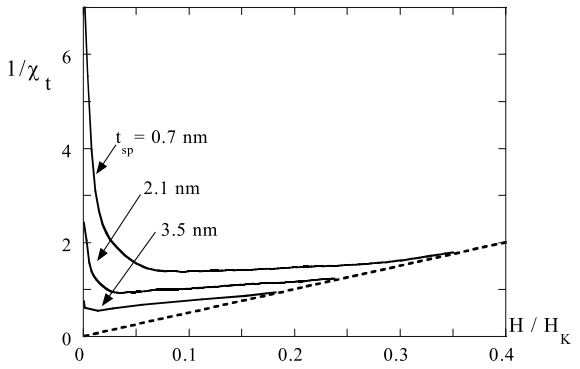

Fig. 10. Variation of $1/\chi_t$ *versus* the amplitude (in reduced units) of the constant field H applied along the stripe. Different curves are plotted according to the thickness of the nonmagnetic spacer t_{sp} of the bilayer system (Co 20 nm/spacer/Co 20 nm). (Quality factor $Q = 0.4$.)

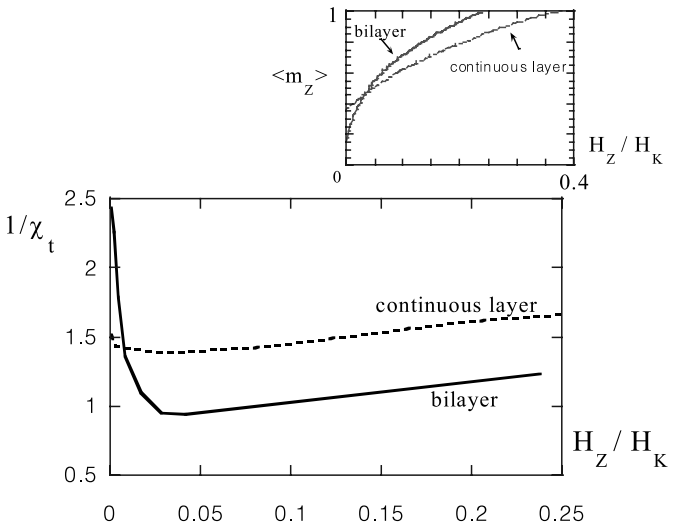

Fig. 11. Comparison of the behaviour of the inverse transverse bias susceptibility: $1/\chi_t$ under a in-plane applied field H_Z for: a bilayer (Co 20 nm/spacer $t = 2$, 1 nm/Co 20 nm) and a continuous magnetic layer 42.1 nm thick. The inset shows the corresponding behaviour for the longitudinal magnetization component $\langle m_Z \rangle$ in these two cases.

elongation of the stripe is shown in Figure 10. In abscissa, the field is expressed in reduced units with respect to the anisotropy field identical for the three bilayers analysed. These bilayers differ by the sole value of the thickness of their non-magnetic spacer. Similar as for single films, the lower is $\langle m_Z \rangle$ of a given bilayer (see Fig. 7 in Ref. [14]) the higher is its inverse transverse susceptibility. However, its field dependence is quite different. For $H/H_K > 0.1$, $1/\chi$ increases slightly with H, like in continuous layers and it joins the dashed line in Figure 10 which corresponds to the curve $1/\chi = 4\pi Q H/H_K$ characteristic of thin films above the saturation and, in the present situation, of two individual thin films, uniformly magnetized along the dc field H. Now, when H approaches zero $(\chi)^{-1}$ increases drastically: the thinner the spacer is, the stronger the effect is. Although difficult to compare abruptly, such pronounced change was also observed experimentally on multilayers of FeSi/Si with stripe domains [5].

The numerical TBIS results for a single layer 42.1 nm thick ($R_H = 1.1$) and a bilayer [Co 20 nm/spacer 2.1 nm/Co 20 nm] are reported in Figure 11. In low field, these $1/\chi$ behaviours are very different. A crossover is noticed similar to what is observed for the evolution of the longitudinal magnetization component $\langle m_Z \rangle$ (see inset of Fig. 11) already mentioned in reference [14]. In zero field, the magnetic pattern of a bilayer (see Fig. 9) is deeply affected by the presence of the nonmagnetic gap [14]. The configuration shows a pronounced magnetization circulation. However, compared to a continuous film (Fig. 2) one can notice the absence of any inner 180° wall of Bloch type (*i.e.* core of the vortex). The up and down domains are coupled *via* the dipolar field acting through the spacer. In between these main domains, the flux closure is ensured *via* wall structures characterized by their Néel aspect: the magnetization turns in the YOX plane (see the schematic diagram (a) in Fig. 12). Both effects explain that the longitudinal remanent magnetization $\langle m_Z \rangle$ is much lower compared to the continuous film case and roughly equal to zero for $t_{sp} = 0.7$ nm. Under the action of a small transverse field **h**, two mechanisms can be proposed. First, an

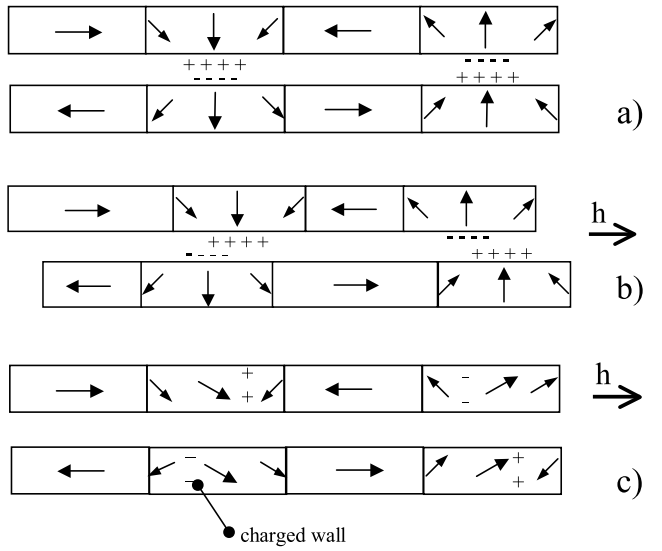

Fig. 12. Schematic representations of the stripe in a bilayer with a very thin nonmagnetic spacer in zero dc field: in a) the dipolar aspect of the coupling is highlighted. b) predicted aspect of the pattern under the action of the small transverse field h assuming volume variation of the closure domains. c) case where a rotation of M is allowed.

increase of the area where M is parallel to h and a corresponding decrease of the region where M is antiparallel. As depicted in Figure 12b this mechanism is locked by the dipolar coupling between the two layers which favours the continuity of the magnetic flux and does try to stabilize the up and down magnetized domain just in front of each other. The second effect concerns a rotation of M which is not possible in the closure domains where M is either parallel or antiparallel to h. Therefore, as far as this mech-

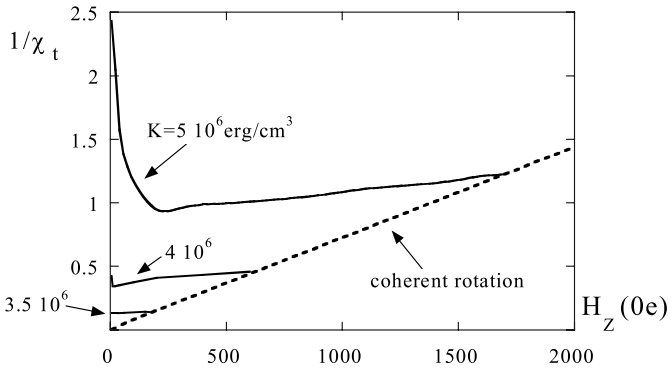

Fig. 13. Variation of $1/\chi_t$ *versus* the amplitude of the constant field H applied along the stripe for the peculiar system (Co 20 nm/spacer 2.1 nm/Co 20 nm) and for different values of the perpendicular anisotropy constant K.

anism is concerned, an infinite value for $(\chi)^{-1}$ is expected. However, the rotation phenomenon could affect the main up and down domains as shown in Figure 12c. Then pronounced inner charged walls (head-to-head walls) would be created what is also forbidden due to the excess of magnetostatic energy needed. Consequently for a very thin spacer the susceptibility should be very weak. However, for thicker spacer, the situation differs. As shown in [14] the remanent magnetization increases quickly with t_{sp} and the area where M_Z is important (zone which can be assimilated to a 180° Bloch wall) is the very zone where a rotation could easily occur under the action of the transverse field (similarly to the previous case of a single layer described in Sect. 3). For such situation a large increase of $(\chi_t)^{-1}$ could be predicted as obtained by numerical simulation.

Finally, we consider the influence of the anisotropy values on the evolution of the inverse susceptibility. Changing perpendicular anisotropy while other magnetic characteristics are kept constant involves, of course, a corresponding variation in the quality factor Q. In Figure 13 are reproduced results for one of investigated bilayers (t_{sp} = 2.1 nm). In the saturated state (large H value), $(\chi)^{-1}$ varies linearly according to the law $(\chi)^{-1} = (1/M)H$. As we have seen before, in low field regime, and for large anisotropy constant ($K = 5 \times 10^6$ erg/cm^3, $Q = 0.4$), $(\chi)^{-1}$ increases abruptly when H decreases towards zero. Such effect disappears for low values of the anisotropy (*i.e.* below a critical anisotropy value) in which case $(\chi)^{-1}$ decreases monotonously with H down to zero field. As there is no in-plane anisotropy, the transverse susceptibility is diverging in zero dc field: even an extremely small transverse applied field, h, is sufficient to align magnetization along its direction. For $H > 0$, the saturated state is got immediately: $\langle m_Z \rangle = 1$ and transverse susceptibility follows the low $(\chi)^{-1} = (1/M)H$ for any field value (dashed line in Fig. 13). Above a critical anisotropy value, the equilibrium magnetic configuration corresponds to a stripe pattern with $\langle m_Z \rangle$ lower than unity but not negligible. For $Q = 0.28$ ($K = 3.5 \times 10^6$ erg/cm^3), the departure from a coherent rotation is quite small. As previously discussed, this means that areas with large $\langle m_Z \rangle$ are strongly coupled to the transverse field and therefore give rise to high susceptibility. Increasing the perpendicular anisotropy progressively aligns the magnetization in the XOY plane and, for $Q > 1$, prevents any rotation of M with h.

5 Conclusion

A full micromagnetic model of stripe domains is developed in order to get a clear insight into the behaviour of transverse bias initial susceptibility as function of dc applied field for thin films and bilayers exhibiting both in-plane and perpendicular anisotropy. It is shown that TBIS can give information about perpendicular anisotropy only in the case if stripe domains are present, *i.e.* above a critical film thickness. Below this critical film thickness (or for lower anisotropy value if the film thickness is kept constant), magnetization remains in the film plane and transverse susceptibility is sensitive only to the in-plane anisotropy. The numerical results are in good agreement with available experimental results for single layers of CoNbZr exhibiting a low quality factor and in which stripe domains are observed. They clearly indicate that the knowledge of the domain pattern is the key to understand the behaviour of the susceptibility. In case of a moderate quality factor, such as in epitaxial cobalt films, it is shown that $(\chi)^{-1}$ has no longer a constant value as found for low Q samples but does increase regularly with the dc field until saturation is reached. Both for low and intermediate Q value, a crude analytical model based on a Landau pattern can be used as a mimic of the real stripe pattern in zero field, and allows to obtain quite easily a reasonable estimation of the TBIS value. As stripe domain pattern is strongly modified by adding a nonmagnetic gap in a bilayer case, this brings up the question about a corresponding change in transverse susceptibility. It is shown that the large divergence of $(\chi)^{-1}$ observed in zero dc field can be attributed to a typical magnetic pattern in the presence of the non-magnetic spacer characterized firstly by the absence of any core of vortices in the magnetic structure, and secondly by a flux closure near the external surfaces, both contributing to prevent rotation of M in a transverse magnetic field. In conclusion, transverse biased initial susceptibility is a sensitive tool to analyse the anisotropy constants in thin films but to get numerical results, it is necessary to take into account the domain pattern and its evolution in applied magnetic fields.

M.L. is very grateful to Dr. Yves Roussigné for enlightening and stimulating discussions on this subject. The authors also acknowledge the assistance of D. Billet (Lab. PMTM-CNRS) for MFM observations.

References

1. E.J. Torok, R.A. White, A.J. Hunt, H.N. Oredson, J. Appl. Phys. **33**, 3037 (1962); E. Feldtkeller, Z. Phys. **176**, 510 (1963)

2. M.C. Contreras, J.F. Calleja, M. Rivas, M.O. Gutiérrez, J.A. Corrales, J. Magn. Magn. Mat. **175**, 64 (1997)
3. J.M. Alameda, M.C. Contreras, H. Rubio, Phys. Stat. Sol. **85**, 511 (1984)
4. G.R. Aranda, J. Gonzalez, O.A. Chubykalo, J.M. Gonzalez, J. Magn. Magn. Mater. **203**, 274 (1999)
5. L.M. Alvarez-Prado, G.T. Pérez, R. Morales, F.H. Salas, J.M. Almeda, Phys. Rev. B **56**, 3306 (1997)
6. R.P. Cowburn, A.O. Adeyeye, M.E. Welland, Phys. Rev. Lett. **81**, 5414 (1998)
7. M. Rivas, J.F. Calleja, M.C. Contreras, J. Magn. Magn. Mater. **53-58**, 166 (1997)
8. H. Hoffmann, Phys. Stat. Sol. **33**, 175 (1969)
9. H. Hoffmann, IEEE. Trans. Magn. **15**, 1215 (1979)
10. R.P. Cowburn, S.J. Gray, J.A.C. Bland, Phys. Rev. Lett. **79**, 4018 (1997)
11. J.M. Alameda, M.C. Contreras, J.F. Fuertes, A. Liénard, F.H. Salas, J. Magn. Magn. Mater. **83**, 75 (1990)
12. J.A. Corrales, M. Rivas, J.F. Callejas, I. Iglesias, M.C. Contreras, J. Appl. Phys. **79**, 5217 (1996)
13. G. Suran, M. Naili, H. Niedoba, F. Machizaud, O. Acher, D. Pain, J. Magn. Magn. Mater. **192**, 443 (1999)
14. M. Labrune, H. Niedoba, Eur. Phys. J. B **27**, 103 (2002)
15. M. Hehn, Ph.D. thesis, University of Strasbourg (1997)
16. M. Labrune, L. Belliard, Phys. Stat. Sol. (a) **174**, 483 (1999)
17. S. Hamada, N. Hosoito, T. Ono, T. Shinjo, J. Magn. Magn. Mater. **198-199**, 496 (1999)
18. A. Hubert, R. Schaefer, *Magnetic Domains* (Springer, London, 1998)